ELSEVIER

International Journal of Mass Spectrometry 222 (2003) 383–396

International Journal of Mass Spectrometry

www.elsevier.com/locate/ijms

Theoretical interpretation of the observed diastereoisomeric differentiation of *cis*- and *trans*-2-methylcyclohexanol in the gas phase mediated by scandium(I)

S. Antonczak[a,*], N. Marchandé[b], D. Cabrol-Bass[a], S. Géribaldi[b]

[a] *Laboratoire Arômes, Synthèses, Interactions, Faculté des Sciences, Université de Nice-Sophia Antipolis, 06 108 Nice Cedex 2, France*

[b] *Laboratoire Chimie des Matériaux Organiques et Métalliques, Faculté des Sciences, Université de Nice-Sophia Antipolis, 06 108 Nice Cedex 2, France*

Received 9 May 2002; accepted 12 September 2002

Abstract

In this study, diastereoisomeric differentiation of *cis*- and *trans*-2-methylcyclohexanol upon reaction with bare scandium cations by means of Fourier transform ion cyclotron resonance (FT-ICR) spectroscopy is reported. Experimental results have shown that the ratio of CH_3ScOH^+ and $HScOH^+$ metalled ions formed is in favor of the former when *cis*-2-methylcyclohexanol is introduced in the system. These results are supported by theoretical computations of relative stabilities and energy barriers of the complexes formed during this reaction. Density functional (DF) calculations performed at the B3LYP/6-31G**//B3LYP/3-21G** level have pointed out that insertion of the Sc^+ cation in the CO or in the OH bonds are energetically competitive with the direct elimination of the cation. From *cis*-2-methylcyclohexanol, formation of CH_3ScOH^+ product proceeds preferentially through insertion mechanisms. Thus, the potential of Sc^+ chemical ionization in the gas phase using FT-ICR spectroscopy could then be extended to the analysis of various alcohols in order to distinguish between diastereoisomers. (Int J Mass Spectrom 222 (2003) 383–396)

Keywords: Scandium; Diasteroisomeric differentiation; Theoretical investigations; Mechanisms

1. Introduction

In last decade, an extensive amount of research has been devoted to the development of mass spectrometric approaches for stereoisomer differentiation [1], particularly using chemical ionization techniques [1–3]. Although the study of mechanistic aspects of the gas-phase chemistry of bare transition metal cations or bare metal oxide cations has attracted considerable interest [4,5], only a few studies deal with the topic of stereoselective gas-phase reactions of these transition metal ions [6]. However, it appears from these works, that metal ion chemical ionization mass spectrometry presents an obvious analytical potential for stereoisomeric differentiation of organic molecules [7].

The hydroxyl group is among the most important functional groups both in chemical and biological compounds. Therefore, when developing methods for stereochemical analysis, cyclic alcohols are often used as model compounds [3,8]. The present study is an

* Corresponding author. E-mail: serge.antonczak@unice.fr

1387-3806/02/$ – see front matter
PII S1387-3806(02)01000-X

effort to explore the potential of Sc^+ chemical ionization in the gas phase for cyclic alcohol diastereoisomeric differentiation. *cis*- and *trans*-2-Methylcyclohexanols have been retained as model compounds. Fourier transform ion cyclotron resonance (FT-ICR or FT-MS) mass spectrometer experiments have been used as analytical tools and theoretical calculations have been performed to try to enlighten the reaction mechanisms involved in this differentiation. Indeed in previous works, we had demonstrated that rare earth metal cations, such as Sc^+, Y^+, and Lu^+ exhibit impressive gas-phase reactivity vs. aliphatic alcohols [9], and that the nature of primary and subsequent products is largely dependent on the aliphatic chain length [10]. For instance, primary reaction of these metal cations M^+ with propan-1-ol leads to $HMOH^+$ and CH_3MOH^+ ions among others, while ethanol leads only to $HMOH^+$ ions. The formation of these ions is summarized in Scheme 1, and has been explained by the intervention of 4- or 5-centers electrocyclic mechanisms in which a competitive β-hydrogen or methyl group transfer occurs [10].

Moreover, in their study of the C–H bond activation of cyclohexane by bare first-row transition metal cations Sc^+–Zn^+, Schwarz and co-workers [11] have shown that the first dehydrogenation occurs stereospecifically in terms of a *syn* elimination. Thus, from these two observations, one can think that the activation reaction of *cis*- and *trans*-2-alkylcycloalkanols by rare earth cations Sc^+, Y^+, and Lu^+, and more particularly *cis*- and *trans*-2-methylcyclohexanols in this work, must lead to proportions of $HMOH^+$ and CH_3MOH^+ being dependent on the stereochemistry of the alcohols (Scheme 2), the *cis* diastereoisomer giving a greater proportion of CH_3MOH^+ ion than the *trans* isomer, and conversely for the $HMOH^+$ ion.

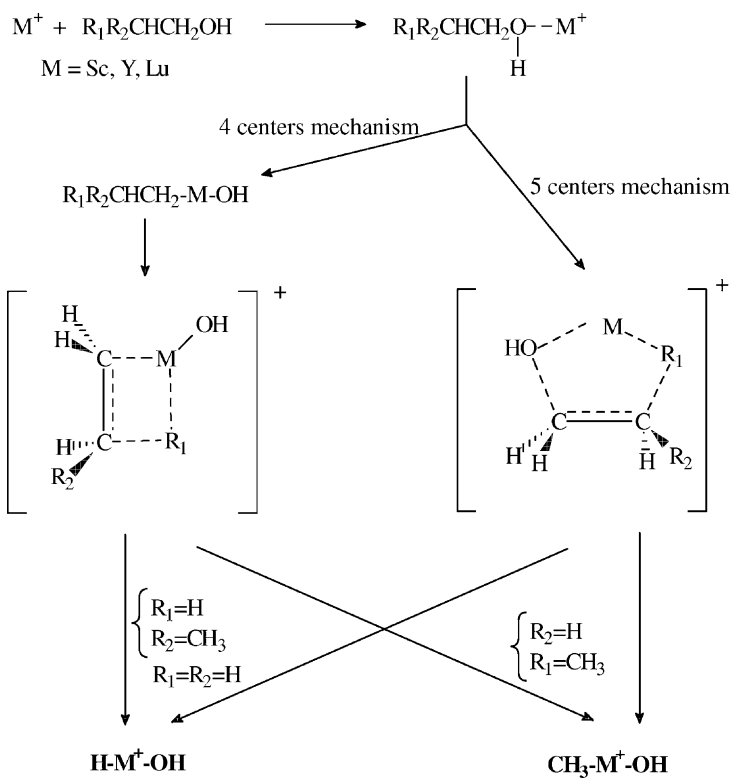

Scheme 1.

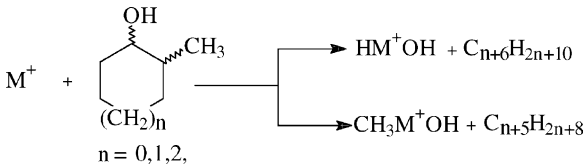

Scheme 2.

Experimental and theoretical descriptions of bonds involving scandium cation and various heteroatoms, such as O [12,13], N [12,14], and S [15], have been recently reported. Some aspects of the ScC [16] and ScSc [17] bonds have also been theoretically investigated. These studies lead to the conclusion that density functional (DF) methods give good results, comparable to classical post-HF calculations with respect to the geometries and the relative energies of a number of molecular systems. Thus, the criteria for the selection of Sc^+ in this preliminary study was that this metal ion has been the subject of numerous theoretical studies [12–18], and at the present its parametrization for theoretical calculations is easier than that of Lu^+ or Y^+ [19].

In the following description is presented a study of the reactions of bare scandium cation with the two stereoisomers *cis*- and *trans*-2-methylcyclohexanol. FT-ICR analyses have shown that the ratio of $HScOH^+$ and CH_3ScOH^+ products is dependent of the conformation of the alcohol. DF calculations have confirmed that a favored reaction path lead preferentially to the formation of the CH_3ScOH^+ product when possible.

2. Experimental

2.1. FT-ICR mass spectrometry experiment

The experiments were performed on an FT-ICR mass spectrometer constructed in part in our laboratory [20]. Complete descriptions of the apparatus and experimental procedures are given elsewhere [9,10].

Scandium ions were generated by laser desorption–ionization [21] by focusing the beam of nitrogen pulsed laser (model VSL 337ND, Laser Science Inc., Newton, MA) onto a pure metal target (>99%, from Alfa Johnson Matthey, Karlsruhe, Germany) placed close to the FT-ICR cell. The *cis*-2-methylcyclohexanol (98%) and the *trans*-2-methylcyclohexanol (99%) were obtained commercially from Sigma–Aldrich. The reactant gases were purified by freeze–pump–thaw cycling. The neutral (*cis*- or *trans*-2-methylcyclohexanol) was introduced in the system via a variable leak valve. A continuous flow was used and adjusted so that the base pressure of neutral was stable on the range $1–4 \times 10^{-5}$ Pa.

For the general procedure, the reactant metal ions were isolated selectively by double-resonance technique [22] and/or frequency sweep excitation [23] to remove all other ions in the cell. The widths and the intensities of ejection and excitation pulses were optimized to minimize the translation activation of the reactant ions [24]. These reactant ions were then stored in the cell and allowed to react with the chosen alcohol. Reaction times are varied by a programmable delay event from a minimum of 0.0014 s to a maximum of 8 s prior to ion detection, allowing both primary and sequential reaction products to be observed. The kinetic analysis of the exponential fall of the reactant ion Sc^+ was performed to determine its decay rates, and also to know if the formed ions come from primary or subsequent reaction.

2.2. Computational methods

It is now generally accepted that DF methods are well suited for the study of such complexes involving transition metals. Preliminary calculations have confirmed that classical ab initio post-HF methods, still remain too demanding in terms of computational time. DF methods seem to be a good option for the study of such systems in which a metal and an fairly large number of heavy atoms are involved. We have chosen the B3LYP method [25] which uses gradient corrected functional of Becke and the correlation functional proposed by Lee et al. [26].

Geometry optimizations have been performed at the B3LYP/3-21G** level [27]. In order to obtain refined energies, single points calculations have been done at

the B3LYP/6-31G** level [28] using B3LYP/3-21G** optimized geometries. These calculations will be denoted B3LYP/6-31G**//B3LYP/3-21G** as usual. To compare the conformational stability of the different complexes, some additional calculations have been performed the B3LYP/3-21G level. This level of calculation leads to an energetical ranking in good agreement with the results found at higher levels of computation. Therefore, unless noticed, all the geometrical parameters presented in the following have been obtained at the B3LYP/3-21G** level while energy differences as well as net atomic charges are given at the B3LYP/6-31G**//B3LYP/3-21G** level of calculation. Thermodynamic corrections [29], calculated at 298 K and 1 atm using B3LYP/3-21G** vibrational frequencies of the optimized structures have been added to the absolute energies. In the following, when noted ΔG, the given energies take into account these corrections. This approximation as well as the chosen level of calculation have been proved to be in good agreement with results obtained at a higher level of calculation. This point will be developed in a forthcoming publication. Transition states have been characterized using Schlegel's algorithm [30] and have been checked to present only one imaginary frequency. By means of the IRC algorithm [31,32], it has been verified that the stationary points located on each side of a transition state are indeed the structures obtained by following the characteristic normal vibration mode of the TS. All the calculations have been performed using the Gaussian 98/DFT program [33].

The following notations are used concerning the *cis*- and *trans*-2-methylcyclohexanol. They only concern the chair conformers since they are the most stable, as explained in the following. A three letters code has been used. The first one denotes the type of molecule: **R** for the reactants, **C** and **O** for the complexes in which the scandium is inserted between the carbon and the oxygen atoms and between the oxygen and the hydrogen atoms, respectively (see Scheme 3). The next two letters code for the methyl and hydroxyl groups orientations, respectively (**A** for axial; **E** for equatorial). For example, **CAE** denotes the complex in which the scandium is inserted between the carbon and the oxygen atoms and where the methyl and the hydroxyl groups are in axial and equatorial orientations, respectively.

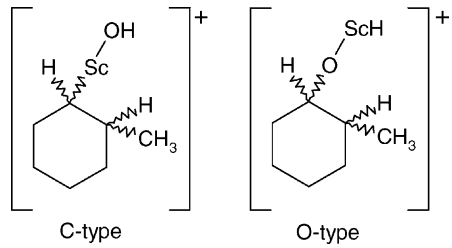

Scheme 3.

3. Results and discussion

3.1. Experimental results

3.1.1. Primary products of the Sc^+ chemical ionization of the 2-methylcyclohexanol as a function of the stereochemistry cis or trans of the alcohol

The branching ratio of primary products, calculated by allowing for the subsequent reactions for the metal ion Sc^+, are reported in Table 1. It appears that the proportions of all the primary products are depending on the stereochemistry of the studied alcohol. Taking into account the number of primary products observed, and consequently, the relatively small proportions of these ions in the primary reaction mixture, the experiments have been performed using different pressures of neutral in the ICR cell. The branching ratios are invariable whatever the pressure used between the range 1×10^{-5} and 4×10^{-5} Pa. Thus, the relative proportions of the two ions under investigation, $HScOH^+$ and CH_3ScOH^+, can be calculated. For the *cis* diastereoisomer, the relative proportions are 22 and 78% for the $HScOH^+$ and CH_3ScOH^+, respectively, while for the *trans* isomer they are 60 and 40%, respectively. These results allow us to confirm our assumptions concerning the potentiality of rare earth metal chemical ionization method to differentiate diastereoisomeric-substituted cyclic alcohols by mass spectrometry. Moreover, these results agree

Table 1
Primary ion–molecule reaction products of Sc^+ with the diastereoisomeric alcohols

Metal ions formed	Neutrals lost	Percent product distribution from	
		cis-2-Methylcyclohexanol	*trans*-2-Methylcyclohexanol
ScO^+	C_7H_{14}	30	44
$ScOH^+$	C_7H_{13}	17	22
$HScOH^+$	C_7H_{12}	4 (22)	9 (60)
CH_3ScOH^+	C_7H_{10}	14 (78)	6 (40)
$ScOC_6H_6^+$	$CH_4 + 2H_2$	9	3
$ScOC_7H_8^+$	$3H_2$	26	14

In parenthesis the relative proportions of $HScOH^+$ and CH_3ScOH^+ ions are given.

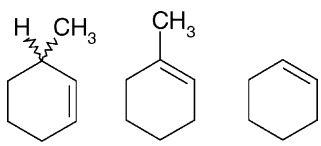

P1 **P2** **P3**

Scheme 4.

with electrocyclic activation mechanisms previously proposed that can be now supported by our theoretical investigations.

3.2. Theoretical results

3.2.1. Position of the problem

In order to correlate the stereochemistry of the reagents with the mass experiments products formation, two scandium complexes are important, namely $HScOH^+$ and CH_3ScOH^+. By elimination of these fragments, three other products can be obtained and will be denoted **P1**, **P2**, and **P3** (see Scheme 4).

Energy comparison shows unambiguously that **P3** + CH_3ScOH^+ is the more stable pair of products. **P2** + $HScOH^+$ and **P1** + $HScOH^+$ are found to be 13.7 and 17.0 kcal mol^{-1} higher in energy, respectively (see Scheme 4). Thermodynamic corrections increase only slightly these energy values (0.4 and 0.8 kcal mol^{-1}, respectively). It is clear that the energetic difference is in favor of the formation of the **P3** + CH_3ScOH^+ pair of products (see Table 2) from the separate reactants. However, for a better understanding of the diastereoisomeric differentiation abovementioned, the whole mechanisms need to be elucidated.

3.2.2. General overview of the investigated mechanisms

The mechanisms described in this work do not take into account the possible reactions between two fragments already dissociated but focus only on reactions involving the same number of atoms from the beginning to the end of the mechanism. In Scheme 5 is presented a general overview of the potential energy surface (PES) of the formation of the separate

Table 2
Relative energies and free energies (in kcal mol^{-1}) of the three pairs of products with respect to the separate reagents (SR)

		P1 + $HScOH^+$	**P2** + $HScOH^+$	**P3** + CH_3ScOH^+
REE + Sc^+	ΔE	−50.4	−53.7	−67.4
	ΔG	−60.7	−64.3	−78.5
REA + Sc^+	ΔE	−51.9	−55.2	−68.9
	ΔG	−62.3	−65.9	−80.1
RAE + Sc^+	ΔE	−52.6	−55.9	−69.6
	ΔG	−62.6	−66.2	−80.4
RAA + Sc^+	ΔE	−53.2	−56.5	−70.2
	ΔG	−63.7	−67.3	−81.5

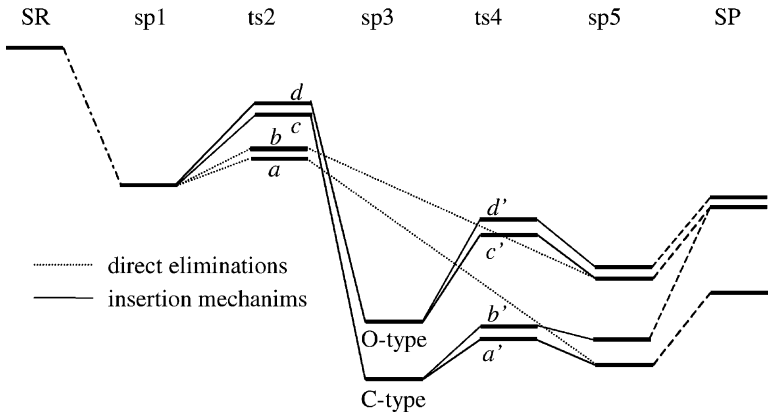

Scheme 5.

products (SP) from the separate reactants (SR). Stable intermediates are denoted as sp for stationary point and transition state as ts. Such a PES exists for the four different 2-methylcyclohexanol isomers. Starting from separate reactants the first step (SR → sp1) consists in the complexation of the scandium cation on the oxygen atom of the hydroxyl group of the methylcyclohexanol compound (see Fig. 1). Since the metal is not yet covalently bonded to the oxygen, the scandium atom (and so the whole sp1 complex) can still be considered as a triplet electronic state. Then, two different reaction paths can be put forward : the scandium cation products formation can either proceed through a direct elimination (see Scheme 1, 5-centers mechanism and Scheme 5, dotted lines), or through a process involving the formation of scandium insertion complexes (see Scheme 1, 4-centers mechanisms and Scheme 5, solid lines). Since the sp1 complex can either be in a singlet or triplet state, the transition states ts2 have been characterized in both states for the two general mechanisms whenever possible. Around these stationary points of the PES, a conical intersection between the triplet state and the singlet state schemes can occur. Indeed, both sp3 and sp5 complexes are more stable in singlet state. For example, $HScOH^+$ and CH_3ScOH^+ are respectively more stable by 56.8 and 42.2 kcal mol^{-1} in singlet state than in triplet state. Furthermore, localization of transition states in triplet state for both the direct eliminations and the insertion mechanisms leads to some convergence problems. Nevertheless, in most cases, described as follows, ts2 transition state absolute energies are in the same range for both open and closed shell schemes. Thus, the conical intersection can occur just before or just after the ts2 transition states. Localizing such a point being not the purpose of this work, the comparison of

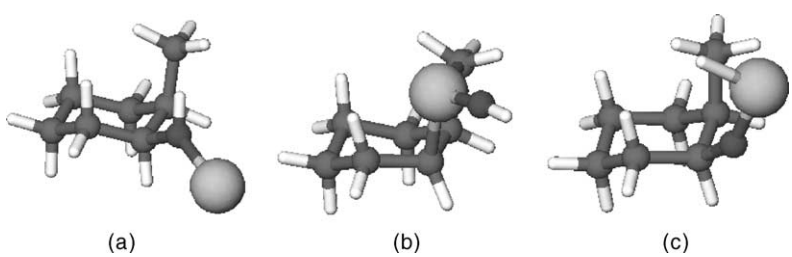

Fig. 1. Structures of the sp1 complexes (a) and of the two sp3 insertion complexes (b and c). Structures (b) and (c) correspond to the **C**- and **O**-type complexes, respectively. This example is given for the **RAE** reagent.

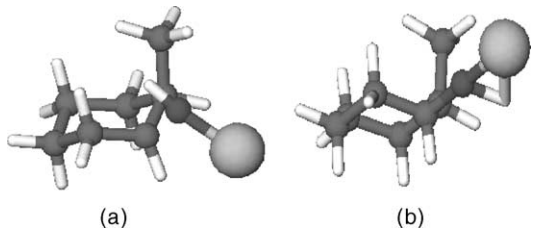

Fig. 2. Structures of the two ts2 transition states for the insertion mechanism in the CO (a) and OH (b) bonds. This example is given for the **RAE** reagent.

those two types of mechanisms (direct or insertion) will mainly be based on the closed shell scheme.

In the direct elimination path, the scandium cation reacts directly with a hydrogen atom or a methyl group bound to the C_β carbon with respect to the hydroxyl group. This transition state leads directly to the sp5 complexes representing the products in electrostatic interaction. In the second mechanism, the scandium is either inserted in the OH bond or in the CO bond (stationary points sp3, see Figs. 1 and 2). Each of these two types of complexes can then lead to elimination transition states where the scandium cation or the oxygen atom reacts with a hydrogen atom placed in β or where the scandium cation reacts with the carbon of the methyl group to form the sp5 product electrostatic complexes (see Figs. 3 and 4).

If one considers only methylcyclohexanol chair conformations, OH and CH_3 groups can then be considered in *cis* or *trans* position (axial and equatorial in the former case and equatorial–equatorial or axial–axial in the latter one). The two *cis* or two *trans* conformations can be respectively inverted in terms of axial and equatorial positions. These inversions proceed through boat conformations which are less stable than chair ones and will not be discussed more deeply in this work. Thus, four different sp1 complexes should be taken into account, leading to eight ts2 transition states in the case of direct elimination and to eight transition states in the case of insertion mechanisms. The eight sp3 complexes can then lead to 14 transition states of elimination (ts4) since in the case of scandium insertion in the OH bond in the *cis* compounds, the elimination is not possible between the O and the CH_3 groups.

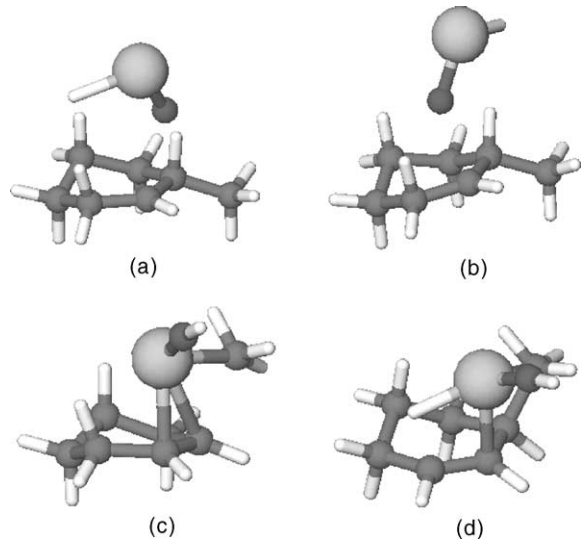

Fig. 3. Structures of the ts4 transition state: (a) and (b) correspond to the elimination of $HScOH^+$ from the **OEE** complex; (c) and (d) correspond to the elimination of CH_3ScOH^+ and $HScOH^+$, respectively, from the **CAE** complex.

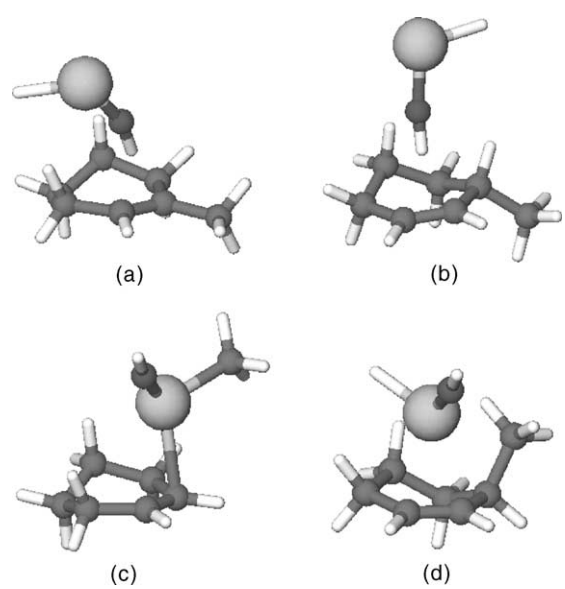

Fig. 4. (a) and (c) Structures of the sp5 electrostatic complexes resulting from the transition state presented in Fig. 3; (b) and (d) lead to the same couple of separate product **P1** + $HScOH^+$.

3.2.3. Reagents

Both *cis*- and *trans*-2-methylcyclohexanol have been considered as reagents. Some calculations performed at the B3LYP/3-21G level have shown that the boat conformations were less stable than the chair ones by at least 7 kcal mol^{-1}. Therefore, in the following, only the latter will be considered. At the B3LYP/6-31G**//B3LYP/3-21G** level of calculation, the **REE** conformation is found to be the most stable. **REA**, **RAE**, and **RAA** are found to be higher in energy by 1.50, 2.2, and 2.8 kcal mol^{-1}, respectively. These energetical differences change only slightly when taking into account the thermodynamic corrections: 1.6, 1.9, and 3.0 kcal mol^{-1}, respectively. Therefore, for each pair of conformers, a slightly more stable structure can be put forward, namely **REE** and **REA**.

3.2.4. Complexation of the scandium atom

On each of these four structures, the scandium cation can be complexed on the oxygen atom of the hydroxyl group (See Fig. 1). In the gas phase, the scandium atom is more stable in its $4s^1 3d^1$ configuration than in its $4s^2 3d^0$ configuration. Therefore, in this work, complexes have been optimized both in singlet and in triplet states. The latter ones are more stable than the former by 7.5, 11.9, 6.5, and 11.5 kcal mol^{-1} for complexes derived from the **REE**, **REA**, **RAE**, and **RAA** reagents, respectively. The four binding energies are in the range of 40–50 kcal mol^{-1}: −41.4, −45.7, −41.1, and −46.8 kcal mol^{-1} from the separate reactants Sc^+ and **REE**, **REA**, **RAE**, and **RAA**, respectively. The nature and strength of the Sc–O bonds will be described in a forthcoming study but it is important to note here that the Mulliken net atomic charge of the scandium cation is roughly +1 in these complexes while the average Sc–O bond length is 2.06 Å.

3.2.5. Direct elimination of the $HScOH^+$ and CH_3ScOH^+ products

From sp1 complexes, CH_3ScOH^+ and $HScOH^+$ cations can be produced by direct elimination reaction involving a 5-centers mechanism. The scandium atom reacts with a hydrogen atom or with the methyl group placed in β as described earlier (see Schemes 1 and 5, dotted lines). Then, six reaction mechanisms can lead to the direct elimination of the $HScOH^+$ cation while only two can lead to the formation of the CH_3ScOH^+ product. Here again, both open and closed shell pathways have been considered. Concerning the open shell scheme, the two transition states leading to the creation of CH_3ScOH^+ cation have been localized while all our attempts to locate these transition states for the mechanisms implying the formation of $HScOH^+$ failed. In the latter case, calculations led to an evolution of the system backward to the respective sp1 complexes. On the other hand, most of the transition states corresponding to the singlet state scheme have been characterized. Only two of these transition states have not been localized : from the **REE** reactant, the direct transition state leading to the **P2** + $HScOH^+$ pair of products and from the **RAE** reactant, the direct transition state leading to the **P1** + $HScOH^+$ pair of products. During the optimization of these transition states, calculations always led to the corresponding sp1 complexes. The corresponding energy values are reported in Table 3. In the singlet state scheme, energy barriers of the paths leading to the $HScOH^+$ cation are less than half as large as the energy barriers of the reaction paths leading to the CH_3ScOH^+ cation (energetic difference of 10–15 kcal mol^{-1} in favor of the creation of the $HScOH^+$ cation). In the latter case, though the free energy barriers for the open scheme are higher, absolute energies of the corresponding transition states remain lower by about 3 kcal mol^{-1} in triplet state than in singlet state (see Table 3). These energies are still high enough to lead to the conclusion that, in the direct elimination, the reaction proceeds preferentially through the elimination of the $HScOH^+$ cation whatever the nature of the reactant. Furthermore, comparison of the energies obtained for open and closed shell mechanisms leading to CH_3ScOH^+ indicates that the intersection between singlet and triplet states adiabatic surfaces should occur after these transition states. Indeed, the resulting complexes are much higher in energy in triplet state than in singlet state. As an example, we have calculated for both

Table 3
Relative energies and relative free energies (in kcal mol^{-1}) of the transition states for the direct elimination processes with respect to the corresponding sp1 structures in the singlet state scheme

	Elimination on	Cation formed	Transition state ts2[a]	
			ΔE	ΔG
REE	The methyl side	$HScOH^+$	Not characterized	Not characterized
	The hydrogen side	$HScOH^+$	16.4	12.6
REA	The methyl side	CH_3ScOH^+	27.6 (35.4)	25.7 (33.9)
	The hydrogen side	$HScOH^+$	12.6	10.2
RAE	The methyl side	CH_3ScOH^+	27.7 (31.7)	25.9 (29.2)
	The hydrogen side	$HScOH^+$	Not characterized	Not characterized
RAA	The methyl side	$HScOH^+$	14.0	11.7
	The hydrogen side	$HScOH^+$	12.9	10.4

In parenthesis the corresponding values for the open shell scheme are given.
[a] ts2 *a* and *b* transition states as described in Scheme 5.

cases the energy of the sp5 complex corresponding to the formation of CH_3ScOH^+ from the **RAE** reactant. In the triplet scheme, absolute energy of this particular stationary point is found to be 44.5 kcal mol^{-1} higher than the corresponding value computed for the singlet state scheme ($\Delta G = 42.2$ kcal mol^{-1}). Furthermore, $HScOH^+$ and CH_3ScOH^+ are respectively more stable by 56.8 and 42.2 kcal mol^{-1} in singlet state than in triplet state. Since, on the triplet state adiabatic surface, no transition states for the direct elimination of $HScOH^+$ has been characterized, no such clear conclusion can be put forward. Nevertheless, this surface has been extensively explored and on this basis, one is justified in thinking that, if these transition states exist, they should be far higher in energy than the corresponding ones in the singlet state scheme. One can then conclude that the surfaces crossing should occur before elimination transition states.

From a structural point of view, the two types of transition states present some significant geometrical differences on scandium side. In the case of the CH_3ScOH^+ cation elimination, the transition state involved in the mechanism can be represented formally as a 5-centers ring structure (see Scheme 5). No major difference exist between the structures localized in open and closed shell schemes except for the Sc–C bond to be formed and for the C–C bond to be broken (respectively 0.15 and 0.08 Å longer in triplet state scheme). Though the ScC bond is not completely formed, the distance is slightly shorter in the transition state structures than in the CH_3ScOH^+ cation (≈2.03 Å vs. 2.10 Å, respectively). In addition, note that the CC bond to be broken is large (1.98 Å) but also that a new interaction arises between the scandium atom and the C_β carbon atom (2.44 Å). These two ScC bond lengths are very close to the values obtained in the structure of the corresponding resulting complex sp5 and, therefore, these transition states can be considered as late TS with respect to these interactions. A contrario, CO and ScO bond lengths (1.54 and 2.07 Å, respectively) do not change in a significant manner from the sp3 complex to the TS (while $d_{ScO} = 1.76$ Å in the CH_3ScOH^+ cation). Same trends are also reported for transition states involved in the direct elimination of the $HScOH^+$ cation: $d_{ScH} \approx 1.78$ Å in the transition states and 1.74 Å in $HScOH^+$; a specific interaction exist between the scandium atom and the C_β (≈2.26 Å). In both transition state types, this particular interaction can justify the relatively short bond length between $ScCH_3$ or ScH and is able to stabilize the structures. These various transition states lead to the corresponding sp5 complexes described later.

3.2.6. *Insertion of the Sc^+ in the CO or OH bonds*

From sp1 complexes, the scandium cation can be inserted either in the OH bond or in the CO bond. In the following, they will be denoted **O**- and **C**-type complexes, respectively (see Scheme 3). All transition

states corresponding to singlet state scheme have been characterized. In the open shell scheme, the four transition states corresponding to the insertion of the scandium cation in the CO bond have been characterized and are found to be 4.0, 4.2, 3.1, and 4.5 kcal mol^{-1} more stable than their homologs in the closed shell scheme for **REE**, **REA**, **RAE**, and **RAA** compounds, respectively. From a structural point of view, the CO bond is being broken while, conversely, the Sc–C bond is being formed (See Fig. 2). Average CO and ScC distances are 2.14 and 3.04 Å, respectively, for closed shell mechanisms. No major structural difference appears for triplet state scheme except that the CO and ScC distances are shorter (average values of 2.04 and 2.75 Å, respectively). Concerning the insertion in the OH bond, only the transition state corresponding to the **REA** compound has been localized but is less stable by 5.7 kcal mol^{-1} than its homolog in the closed shell scheme (see Fig. 2). For the three other conformations, during the transition state localization, the systems tend to return to sp1 structures.

The energetic barriers for the (sp1 → ts2 → sp3) steps of the reactions are reported in Table 4. First, note that though the transition state of the triplet state schemes are lower in energy, the corresponding energetic barriers are higher than those of the singlet state scheme. Then, insertion in the OH bond requires less energy than insertion in the CO bond but, however, the two paths still remain competitive. The major difference in these two paths is reported for the resulting complexes energies. Indeed, complexes in which the scandium cation is inserted in the CO bonds are more stable by about 20 kcal mol^{-1} with respect to the corresponding **O**-type complexes.

For the **C**-type family, the complex in which the methyl group is in equatorial orientation and the group involving the scandium is in axial orientation, namely **CEA**, is the most stable while the **OEE** complex is the most stable in the **O**-type family. Nevertheless, the energetic differences are rather weak in each clan. The **O**-complexes differ at the most by only 2.5 kcal mol^{-1} while this maximum difference reaches 6.0 kcal mol^{-1} when **C**-complexes are considered.

Generally speaking, Sc^+ cation insertion does not lead to important structural modifications of the cycle in **O**-complexes (see Fig. 1). Nevertheless, when possible (**OAA** and **OEA** complexes), the scandium atom is placed close to the axial hydrogen atoms of the cycle, stabilizing the structures. The relevant bond lengths evolve only slightly from one complex to another (mean values: $d_{CO} \approx 1.49$ Å, $d_{OSc} \approx 1.76$ Å, and $d_{ScH} \approx 1.76$ Å). The same trend is reported concerning the net atomic charges for which the mean values are: $q_C \approx +0.16e$, $q_O \approx -0.60e$, $q_{Sc} \approx +1.17e$, and $q_H \approx -0.15e$. Concerning **C**-complexes (see Fig. 1), some important structural modifications can be reported. In order to obtain a maximum stabilization, the scandium atom tends to interact with the

Table 4
Relative energies and relative free energies (in kcal mol^{-1}) of the insertion transition states and the resulting complexes with respect to the corresponding sp1 structures in the singlet state scheme

	Insertion in	Transition states (ts2)[a]		Insertion complexes (sp3)	
		ΔE	ΔG	ΔE	ΔG
REE	The CO bond	13.4 (17.4)	10.9 (14.4)	−58.0	−61.7
	The OH bond	13.7	9.6	−37.4	−42.0
REA	The CO bond	13.1 (21.4)	10.5 (18.2)	−60.6	−64.9
	The OH bond	13.3 (34.2)	9.1 (26.7)	−40.0	−42.7
RAE	The CO bond	14.1 (18.4)	12.5 (16.0)	−60.1	−62.1
	The OH bond	14.3	10.8	−38.1	−40.8
RAA	The CO bond	14.7	12.5 (19.5)	−56.2	−58.7
	The OH bond	14.4	10.6	−38.5	−42.7

In parenthesis the corresponding values for the open shell scheme are given.
[a] ts2 *c* and *d* transition states as described in Scheme 5.

accessible carbon atoms of the cycle or with the carbon atom of the methyl group. Nevertheless, in this family, the pertinent bond lengths also do not change significantly (mean values: $d_{CSc} \approx 2.06$ Å, $d_{ScO} \approx 1.80$ Å, and $d_{OH} \approx 0.96$ Å). Net atomic charges mean values for these complexes are: $q_C \approx -0.32e$, $q_O \approx -0.67e$, $q_{Sc} \approx +1.13e$, and $q_H \approx +0.35e$.

Inspection of net atomic charges of the functional group reveals that the charge of the scandium is higher than formal charge of one electron while the charges of the atoms bound to the metal are strongly negative. This character of the metal atom leads to a functional fragment (OScH or ScOH) much more positively charged in the **C**-complexes than in the **O**-complexes (mean values: $\approx +0.81e$ and $0.40e$, respectively). If one considers the net atomic charge of the carbon atom of the cycle in this count, the charge of the functional group is approximately the same in **C**- and **O**-complexes (mean values: $\approx +0.51e$ and $0.56e$, respectively).

The scandium atom insertion between a carbon atom of the cycle and a hydrogen atom or the methyl group have also been considered. The resulting complexes are less stable than the **C**-type complexes by about 80 and 70 kcal mol^{-1}, respectively (these comparisons and the following are based on calculations performed at the B3LYP/3-21G level of computation). The formation of complexes where the scandium ion is not inserted but only in interaction with the cycle has been taken into account. When the Sc^+ interacts on the side of the cycle where the hydroxyl group is not accessible, the complex is less stable than the **C**-type complexes by about 100 kcal mol^{-1}. Therefore, this possibility can be ruled out.

3.2.7. *Elimination of the CH_3ScOH^+ and $HScOH^+$ products*

Charged CH_3ScOH^+ and $HScOH^+$ species and **P1**, **P2**, and **P3** neutrals formation can only occur through a 4-centers mechanism (see Scheme 1). Each **O**- and **C**-type complexes can lead to the scandium elimination through the formation of **P1** and $HScOH^+$ products (see Table 5 for the possible eliminations and the respective energies). A contrario, only **OAA**, **OEE**, **CAA**, and **CEE** complexes can lead to the pair of products **P2** and $HScOH^+$. Finally, only the two complexes **CAE** and **CEA** can lead to the **P3** and CH_3ScOH^+ pair of products.

Inspection of the values given in Table 5 shows that some intermediates having the boat conformation can exist on the PES for some reaction paths. These intermediates have been characterized by following the transition state characteristic normal vibration modes. These structures are higher in energy than the corresponding **O**- and **C**-type complexes. In these boat forms, the ScOH or OScH groups are adequately placed to react with the hydrogen atom or the methyl group placed in β.

Concerning ts4 transition states (see Fig. 3), a very large difference is reported between transition energies necessary to form sp5 complexes from insertion complexes. Indeed, while the average barrier is around 8–9 kcal mol^{-1} for reactions occurring from **C**-type complexes (a' and b' ts4 transition states, see Scheme 5), the same quantities rise 39–40 kcal mol^{-1} for the reactions occurring from **O**-type complexes (c' and d' ts4 transition states, see Scheme 5). This difference is only slightly lowered by addition of the thermodynamical corrections. Furthermore, sp5 complexes formed from **O**-type structures remain higher in energy by about 10 kcal mol^{-1} than the **O**-type insertion complexes. On the other hand, **C**-type structures lead to two different family of complexes depending on the nature of the eliminated ion. When $HScOH^+$ is eliminated, the resulting sp5 complexes are higher in energy than the corresponding sp3 structures by about 5–9 kcal mol^{-1} (b' ts4 transition states, see Scheme 5). But when CH_3ScOH^+ is eliminated, resulting complexes are slightly more stable than sp3 structures by about 4 kcal mol^{-1}. This difference is enhanced by addition of the thermodynamic corrections and reaches 7–9 kcal mol^{-1}.

From a structural point of view, some major discrepancies can be put forward between elimination reactions from **C**- and **O**-type of complexes. Transition states corresponding to the elimination from **C**-type complexes can be considered as late transition states since their structures are quite similar to the

Table 5
Relative energies and relative free energies (in kcal mol^{-1}) of the elimination transition states from the **O**- and **C**-type complexes and the resulting sp5 complexes given with respect to the sp1 structures in the singlet state scheme (see text for notation)

	Reaction on the	Boat intermediate[a]		Transition state ts4		Complexes sp5	
		ΔE	ΔG	ΔE	ΔG	ΔE	ΔG
OEE	Methyl side	–	–	1.3	−8.9	−24.8	−33.3
	Hydrogen side	−34.2	−36.6	2.2	−7.9	−21.3	−29.4
OEA	Methyl side[c]	–	–	–	–	–	–
	Hydrogen side	–	–	1.0	−8.6	−23.0	−31.0
OAE	Methyl side[c]	–	–	–	–	–	–
	Hydrogen side	–	–	2.6	−6.2	−21.7	−29.2
OAA	Methyl side	−32.3	−37.0	0.3	−9.2	−27.0	−35.3
	Hydrogen side	–	–	1.9	−7.4	−22.4	−30.7
CEE	Methyl side	–	–	−49.6	−55.4	−50.1	−57.9
	Hydrogen side	–	–	−47.2	−52.9	−55.1	−61.8
CEA	Methyl side	–	–	−49.0	−52.7	−64.4	−71.9
	Hydrogen side	−57.0	−59.8	−43.7	−49.1	−53.6	−59.0
CAE	Methyl side	–	–	−48.6	−52.2	−64.0	−71.4
	Hydrogen side	–	–	−46.4	−51.2	−51.9	−57.3
CAA	Methyl side	_[b]	_[b]	_[b]	_[b]	_[b]	_[b]
	Hydrogen side	−55.3	−58.4	−45.4	−50.4	−52.3	−58.2

[a] Reaction intermediates in the boat conformation localized in the course of the mechanism.
[b] Reaction path not characterized.
[c] No elimination reaction possible (see text).

corresponding sp5 ones (see Figs. 3 and 4, structures c and d). For example, the ScH transition distance is about 1.81 Å in ts4 structures and about 1.75 Å in the sp5 complexes. The CH bond still exists in the TS but is greatly weakened ($d_{CH} \approx 1.8$ Å). The ScC distance has an average value of 2.25 Å, slightly longer than in the corresponding sp3 structures and slightly shorter than in sp5 complexes (≈2.05 and 2.42 Å, respectively). Conversely, transition states corresponding to the elimination from **O**-type complexes can be considered as early transition states with respect to hydrogen transfer (see Figs. 3 and 4, structures a and b); d_{OH} is about 1.8 Å in ts4 transition structures and about 0.96 Å in sp5 complexes; d_{CH} is about 1.15 and 2.0 Å in ts4 and sp5 structures, respectively; d_{CO} evolves from a value of ≈1.5 Å in sp3 to ≈2.5 Å in ts4 and does not interact with any carbon atom in sp5 structures.

The last steps of the reactions consist in the products separation from the electrostatic sp5 complexes (see Fig. 4) and in an increase of the respective energies. But here again, this increase is in favor of the formation of the CH_3ScOH^+ ion and **P3** neutral.

4. Summary and conclusions

For all these reactions, the first step (sp1 → ts2), reflecting the competition between the two general mechanisms (see Scheme 5, dotted and solid lines) shows unambiguously that direct elimination of the CH_3ScOH^+ cation is not favored for both singlet or triplet state schemes. Indeed, in closed shell direct elimination of the $HScOH^+$ cation requires less energy and, both in closed and open shell, insertion transition states are far lower in energy than the direct elimination of CH_3ScOH^+. Considering these particular paths, only the scandium insertion in the CO bond can formally lead to the formation of CH_3ScOH^+. The two types of insertion transition states (either in the OH or in the CO bond) are competitive, both in singlet or triplet state but the energetic differences for the resulting complexes play in favor of the **C**-type structures (insertion in the CO bond). Furthermore, transition energies corresponding to the formation of the cations from **C**-type complexes are lower than from **O**-type complexes and thus favored (Scheme 5, ts4 state, a'

and b' structures vs. c' and d' ones). Energetic comparison of the two a' and b' transition states points out that formation of CH_3ScOH^+ cation requires less energy than formation of the $HScOH^+$ cation. Finally, separation of the products is energetically in favor of the **P3**+ CH_3ScOH^+ pair rather than the **P1** + $HScOH^+$ and **P2** + $HScOH^+$ pairs. Nevertheless, the preferential reaction path (sp1 → ts2 c → **C** − type sp3 → ts4 a' → sp5 → **P**3+CH_3ScOH^+) is possible only when the reactant is the *cis*-2-methylcyclohexanol (namely **RAE** or **REA**). Note also that, even if energetic considerations are in favor of formation of these products, on each step of the overall mechanism, some more or less competitive reactions could occur. Therefore, the formation of CH_3ScOH^+ is not exclusive.

Some other reactions, that involve on one hand an ScOH fragment for example and methylcyclohexanol reactant or a corresponding radical molecule on the other hand, could also be competitive and, therefore, lead for both types of reactant (*cis*- and *trans*-2-methylcyclohexanol) to both $HScOH^+$ and CH_3ScOH^+ cations. For example, calculations about these fragmentations have been performed at the B3LYP/6-31G**//B3LYP/3-21G** level of computation. In the singlet state scheme, from the sp1 complex formed from the REA reactant, the dissociation energy to form the ScOH and C_7H_{13} fragments is 25.8 kcal mol^{-1}. This energy is in the same range that direct elimination of the CH_3ScOH^+ cation and thus, higher in energy by roughly 15 kcal mol^{-1} than insertion transition barriers. Furthermore, **CEA** and **OEA** complexes are more stable by 90.6 and 65.8 kcal mol^{-1} than ScOH and OScH and the corresponding radicals, respectively.

Lastly, both experimental and theoretical investigations lead to the conclusion that diastereoisomeric differentiation of *cis*- and *trans*-2-methylcyclohexanol is feasible under reaction with bare scandium cation. Indeed, though Sc^+ cation can be inserted in the course of the reaction either in the CO or in the OH bond, it appears theoretically that the insertion in the CO bond is energetically favored. The resulting complex can then lead to the **P3** + CH_3ScOH^+) pair of products when the methyl group and the ScOH fragment are in *cis* conformation. This pair is also thermodynamically favored with respect to the two additional couples of products that can be obtained. Reaction of bare scandium cation with *cis*-2-methylcyclohexanol leads preferentially to the formation of the CH_3ScOH^+ product while the reaction with *trans*-2-methylcyclohexanol leads exclusively to the formation of the $HScOH^+$ product.

Acknowledgements

The author acknowledges greatly the IDRIS Computing Center for the kind help of their technical staff and for the provision of computer resources.

References

[1] J.S. Plitter, F. Turecek, Applications of Mass Spectrometry to Organic stereochemistry, VCH Publishers, New York, 1994.
[2] (a) C. Guenat, D. Houriet, D. Stahl, J. Winkler, Helv. Chim. Acta 68 (1985) 1647;
(b) T. Keough, Org. Mass Spectrom. 19 (1984) 551;
D. Despeyroux, R.B. Cole, J.-C. Tabet, Org. Mass Spectrom. 27 (1992) 300;
(c) W.J. Meyerhoffer, M.M. Bursey, Org. Mass Spectrom. 24 (1989) 246;
(d) Y.-P. Tu, G.-Y. Yang, S.-N. Liu, S.-N. Chen, Y.-Z. Chen, Org. Mass Spectrom. 26 (1991) 645;
(e) Y.-P. Tu, Y.-Z. Chen, S.-N. Chen, M.-L. Wang, Z.-Z. Jing, Org. Mass Spectrom. 25 (1990) 9;
(f) H.F. Grützmacher, K.H. Fechner, Tetrahedron 27 (1971) 5011;
T. Partanen, P.J. Mälkönen, P. Vainiotalo, J.J. Vepsäläinen, Chem. Soc. Perkin Trans. 2 (1990) 777.
[3] (a) D.T. Leeck, T.D. Ranatunga, R.L. Smith, T. Partanen, P. Vainiotalo, H.I. Kenttämaa, Int. J. Mass Spectrom Ion Processes 141 (1995) 229;
(b) K.K. Thoen, L. Gao, T.D. Ranatunga, P. Vainiotalo, H.I. Kenttämaa, J. Org. Chem. 62 (1997) 8702.
[4] (a) P.B. Armentrout, Gas phase organometallic chemistry, in: J.M. Brown, P. Hofmann (Eds.), Organometallic Bonding and Reactivity, Topics in Organometallic Chemistry, vol. 4, Springer-Verlag, Berlin, 1999, p. 1;
(b) K. Eller, H. Schwarz, Chem. Rev. 91 (1991) 1121;
(c) K. Eller, Coord. Chem. Rev. 126 (1993) 93.
[5] D. Schröder, H. Schwarz, Angew. Chem. Int. Ed. Engl. 34 (1995) 1973.
[6] (a) C.A. Schalley, D. Schröder, H. Schwarz, J. Am. Chem. Soc. 116 (1994) 11089 (and references therein);
(b) G. Hornung, D. Schröder, H. Schwarz, J. Am. Chem. Soc. 117 (1995) 8192;

(c) C.A. Schalley, D. Schröder, H. Schwarz, Organometallics 14 (1995) 317;
(d) G. Hornung, D. Schröder, H. Schwarz, J. Am. Chem. Soc. 1197 (1997) 2273.
[7] D. Schröder, C. Heinemann, W. Koch, H. Schwarz, Pure Appl. Chem. 69 (1997) 273.
[8] T.K. Majumdar, F. Clairet, J.-C. Tabet, R.G. Cooks, J. Am. Chem. Soc. 114 (1992) 2897.
[9] M. Azzaro, S. Breton, M. Decouzon, S. Geribaldi, Int. J. Mass Spectrom. Ion Processes 128 (1993) 1.
[10] S. Geribaldi, S. Breton, M. Decouzon, M. Azzaro, J. Am. Chem. Soc. Mass Spectrom. 7 (1996) 1151.
[11] K. Seemeyer, D. Schröder, M. Kempf, O. Lettau, J. Müller, H. Schwarz, Organometallics 14 (1995) 4465.
[12] G.P. Kushto, M. Zhou, L. Andrews, C.W. Bauschlicher, J. Phys. Chem. A 103 (1999) 1115.
[13] C.W. Bauschlicher, M. Zhou, L. Andrews, J.R. Tobias Johnson, I. Panas, A. Snis, B.J. Roos, J. Phys. Chem. A 103 (1999) 5463.
[14] T.C. Steimle, J. Xin, A.J. Marr, S.J. Beaton, Chem. Phys. 106 (1997) 9084;
G.V. Chertihin, L. Andrews, C.W. Bauschlicher, J. Am. Chem. Soc. 120 (1998) 3205.
[15] I. Kretzschmar, D. Schröder, H. Schwarz, C. Rue, P.B. Armentrout, J. Phys. Chem. A 104 (2000) 5046.
[16] M.C. Holthausen, C. Heinemann, H.H. Cornehl, W. Koch, H.J. Schwarz, Chem. Phys. 102 (1995) 4931.
[17] C.J. Barden, J.C. Rienska-Kiracofe, H.F. Schaefer III, J. Chem. Phys. 113 (2000) 690.
[18] (a) K.C. Crellin, J.L. Beauchamp, W.A. Goddard III, S. Geribaldi, M. Decouzon, Int. J. Spectrom. Ion Processes 182/183 (1999) 121;
(b) J.K. Perry, W.A. Goddard III, J. Am. Chem. Soc. 116 (1994) 5013;
(c) C.W. Bauschlicher Jr, S.R. Langhoff, Int. Rev. Phys. Chem. 9 (1990) 149;
(d) T.F. Magnera, D.E. David, J. Michl, J. Am. Chem. Soc.111 (1989) 4100;
(e) L.F. Halle, W.E. Crowe, P.B. Armentrout, J.L. Beauchamp, Organometallics 3 (1984) 1694.
[19] A. Ferhati, Ph.D. thesis, University of Paris-Sud, 1994.
[20] M. Decouzon, J.-F. Gal, S. Geribaldi, P.-C. Maria, M. Rouillard, Spectra 2000 17 (1989) 51.
[21] (a) B.S. Freiser, Anal. Chim. Acta 178 (1985) 137;
(b) B.S. Freiser, Talanta 32 (1985) 697.
[22] L.R. Anders, J.L. Beauchamp, R.C. Dunbar, J.D. Baldeschwieler, J. Chem. Phys. 45 (1966) 1062.
[23] M.B. Comisarow, A.G. Marshall, Chem. Phys. Lett. 25 (1974) 489.
[24] S. Murthy, J.L. Beauchamp, J. Phys. Chem. 96 (1992) 1247.
[25] (a) A.D. Becke, J. Chem. Phys. 98 (1993) 5648;
(b) P.J. Stephens, F.J. Devlin, C.F. Chabalowski, M.J. Frisch, J. Phys. Chem. 98 (1994) 11623.
[26] C. Lee, W. Yang, R.G. Parr, Phys. Rev. B 37 (1988) 785.
[27] K.D. Dobbs, W.J. Hehre, J. Comput. Chem. 8 (1987) 86.
[28] V. Rassolov, J.A. Pople, M. Ratner, T.L. Windus, J. Chem. Phys. 109 (1998) 1223.
[29] W.J. Hehre, L. Radom, P.v.R. Schleyer, J.A. Pople, Ab Initio Molecular Orbital Theory, Wiley, New York, 1986, p. 226.
[30] H.B. Schlegel, J. Comput. Chem. 3 (1982) 214.
[31] C. Gonzalez, H.B. Schlegel, J. Chem. Phys. 90 (1989) 2154.
[32] C. Gonzalez, H.B. Schlegel, J. Chem. Phys. 94 (1990) 5523.
[33] M.J. Frisch, G.W. Trucks, H.B. Schlegel, G.E. Scuseria, M.A. Robb, J.R. Cheeseman, V.G. Zakrzewski, J.A. Montgomery Jr., R.E. Stratmann, J.C. Burant, S. Dapprich, J.M. Millam, A.D. Daniels, K.N. Kudin, M.C. Strain, O. Farkas, J. Tomasi, V. Barone, M. Cossi, R. Cammi, B. Mennucci, C. Pomelli, C. Adamo, S. Clifford, J. Ochterski, G.A. Petersson, P.Y. Ayala, Q. Cui, K. Morokuma, D.K. Malick, A.D. Rabuck, K. Raghavachari, J.B. Foresman, J. Cioslowski, J.V. Ortiz, A.G. Baboul, B.B. Stefanov, G. Liu, A. Liashenko, P. Piskorz, I. Komaromi, R. Gomperts, R.L. Martin, D.J. Fox, T. Keith, M.A. Al-Laham, C.Y. Peng, A. Nanayakkara, C. Gonzalez, M. Challacombe, P.M.W. Gill, B. Johnson, W. Chen, M.W. Wong, J.L. Andres, C. Gonzalez, M. Head-Gordon, E.S. Replogle, J.A. Pople, Gaussian 98, Revision A.7, Gaussian, Inc., Pittsburgh PA, 1998.